University Library

A gateway to Melbourne's research publications

Minerva Access is the Institutional Repository of The University of Melbourne

Author/s:
Lu, Z;Yang, Y;Brear, MJ

Title:
Impact of ethanol on oxidation of iso-octane at low and intermediate temperatures

Date:
2020-04-01

Citation:
Lu, Z., Yang, Y. & Brear, M. J. (2020). Impact of ethanol on oxidation of iso-octane at low and intermediate temperatures. Combustion and Flame, 214, pp.167-183. https://doi.org/10.1016/j.combustflame.2019.12.040.

Persistent Link:
https://hdl.handle.net/11343/240983

Impact of Ethanol on Oxidation of Iso-Octane at Low and Intermediate Temperatures

Zhewen Lu, Yi Yang* and Michael J. Brear

Department of Mechanical Engineering
The University of Melbourne, Parkville VIC 3010 Australia

Abstract

This paper investigates the impact of ethanol on the oxidation of iso-octane at low and intermediate temperatures. Flow reactor experiments are conducted on binary mixtures ranging from neat iso-octane to neat ethanol at temperatures of 650 K and 875 K, a pressure of 10 bar and an equivalence ratio of 0.058, with the intermediate species and gas temperatures measured along the reactor. At 650 K, where neat iso-octane is near the peak of its low temperature chain branching, the addition of small amounts of ethanol dramatically suppresses iso-octane's reactivity and formation of intermediate species. Kinetic simulation reveals that this inhibition effect is a result of ethanol competing for OH radicals and producing an imbalance in OH formation, without affecting the iso-octane oxidation mechanism directly or altering its reaction flux distribution. By consuming more OH than it can produce, oxidation of ethanol progressively depletes OH in the radical pool, even at a low blending level, and leads to a strong reduction in the overall reactivity. In contrast, at 875 K, iso-octane and ethanol show comparable reactivities, and the formation of intermediate species correlates roughly linearly with the ethanol content, suggesting negligible interaction between the two fuels at intermediate temperatures. Overall, these results help to explain ethanol's inhibition on the knock propensity of iso-octane in spark ignition engines, as evidenced by the synergistic blending of the two fuels in octane numbers [1].

Keywords: Ethanol, Iso-octane, Low-temperature Oxidation, Flow Reactor, Octane Blending

1. Introduction

Ethanol is the most widely used biofuel and features distinctive qualities that aid the performance of spark-ignition (SI) engines [2–5]. One major benefit is ethanol's strong anti-knock property which is manifested by its high octane number, and which can be utilized to increase the efficiency of SI engines by implementing higher compression ratio and/or more aggressive engine tuning.

However, the octane blending behaviour of ethanol and gasoline is complicated and a linear blending rule often does not apply. The blending of the Research Octane Number (RON) and Motor Octane Numbers (MON) varies not only with ethanol content but also with the octane number and composition of the hydrocarbon blendstocks [1,6–9]. For example, Foong et al. [1] found that the octane blending of ethanol with iso-octane and n-heptane was super-linear (i.e. synergistic) but sub-linear (i.e. antagonistic) with toluene. These non-linearities remain even after ethanol's charge cooling effect is compensated for in the RON measurement [10], inferring strong and fuel-dependent chemical interactions between ethanol and hydrocarbons.

The present work concerns the interaction chemistry of ethanol and iso-octane. As a primary reference fuel, iso-octane has a fixed octane number which is lower than ethanol in RON (100 vs. 109) but higher in MON (100 vs. 91), suggesting that the autoignition reactivities of the two compounds cross at one point. Considering that RON is measured at an engine intake temperature more than 100°C lower than that of MON [11,12], it is expected that iso-octane is more reactive at lower temperatures whereas ethanol is more reactive at higher temperatures.

Several combustion chemistry experiments support this. For example, Song and Song [13] measured the ignition delays of ethanol/iso-octane mixtures in a rapid compression machine (RCM) at 750-900 K and 27 bar. They found that the addition of 0%, 10% and 20% ethanol by liquid volume (referred to as E0, E10 and E20 hereafter) suppressed the reactivity of iso-octane, but this effect weakened as temperature increased. Bogin et al. [14] studied E0, E10, E20, E50 and E100 in an ignition quality tester (623 – 993 K, 5 – 15 bar and ϕ = 0.7 – 1) and measured ignition delays of the fuel sprays. In this diesel-like environment, they found that the reactivities of ethanol and iso-octane cross at temperatures around 850 – 900 K at 10 – 15 bar, which is near the end of the negative temperature coefficient regime for neat iso-octane. A non-monotonic impact of ethanol blending was also observed on the oxidation reactivity, where E20 and E50 were measured with longer ignition delays than ethanol (and iso-octane)

at temperatures below the crossover point. More recently, we used a flow reactor to measure the CO formation from the oxidation of E0, E10, E20, E50, E85 and E100 over 550 – 900 K and at 10 bar [15]. We observed that the reactivities of ethanol and iso-octane crossed at around 775 K. At 650 – 750 K, ethanol strongly suppressed the low-temperature reactivity of iso-octane at as low as 10 vol% blending level, resulting in a non-linear blending for the two fuels. However, as temperature increased, ethanol became more reactive and dominated the CO formation at 900 K when the hot ignition started.

Investigations at higher temperatures have also been reported. Barraza-Botet and Wooldridge [16] conducted RCM experiments at 900-1080 K and 10 atm. for E0, E5, E11, E26, E50, E67 and E100. Due to the temperatures used, neat ethanol was found to be the most reactive fuel in this study. Species measurements and modelling suggested that ethanol and iso-octane reacted independently at these conditions. A similar ignition-promoting effect of ethanol was also reported by Yahyaoui et al. [17] in high-temperature shock tube experiments (1220 – 2315 K, 2 bar), where the addition of ethanol to a gasoline surrogate (50% iso-octane / 35% toluene / 15% 1-hexene by mole %) consistently reduced ignition delays at various blending levels.

Together, these studies demonstrate that the impact of ethanol on iso-octane varies with temperature, and a strong inhibition effect is typically observed at lower temperatures. The kinetic mechanism causing the inhibition effect, however, has not been fully explored. It is noted that similar inhibition effects have been reported for ethanol/n-heptane and ethanol/PRF mixtures [18–23], and the effects have been attributed to the reduced OH formation due to ethanol blending. This mechanism needs to be examined for ethanol/iso-octane mixtures since both iso-octane and ethanol have much lower reactivity than n-heptane and neither produces a significant amount of OH during low temperature oxidation.

This present work therefore investigates the interaction chemistry between ethanol and iso-octane at low and intermediate temperatures using flow reactor experiments and systematic analysis of the reaction chemistry. The objectives are to understand ethanol's strong and contradicting impacts on iso-octane oxidation, which is evidently different from that in ethanol/n-heptane mixtures and most likely also different from that in ethanol/toluene mixtures (the RON and MON of toluene are both higher than that of ethanol). The results will help to explain engine autoignition behaviours of these mixtures and further development of related kinetic models.

2. Experimental and modelling methods

2.1. Pressurised flow reactor

The experiment is conducted in a turbulent pressurised flow reactor at the University of Melbourne. Figure 1 shows the setup of the facility. The reactor is a quartz tube with 25 mm diameter and 1000 mm length, housed in a pressure vessel rated to 50 bar and 1000 K. The fuel and air are pre-heated separately and mixed at the start of the reactor. Fast mixing is achieved by a novel orifice-plate mixer which effectively addressed the reaction initialization problem as described in [24]. Air is supplied from an oil-free compressor with the moisture removed by a refrigeration dryer and is in large excess of stoichiometric conditions to reduce the reaction rate. Liquid fuels are supplied from a pressurized tank and vaporized by hot nitrogen before being injected into the hot air via the mixer. The air flow rate is measured by an in-line flow meter. The fuel flow rate is measured by a Coriolis flow meter and verified by real-time measurement of the fuel tank weight. The reactor pressure is controlled by a back-pressure regulator on the exhaust line of the reactor.

A hot-water cooled sample probe is used to collect gas samples along the centreline of the reactor. The sample probe is equipped with three K-type thermocouples of different junction sizes for gas temperature measurement. This method utilizes the differing radiative losses of each thermocouple and the axisymmetric setup of the reactor and thermocouples to find the local gas temperature without having to rely on the assumption of adiabatic walls or assumed values for wall emissivity and convection heat transfer coefficients. The uncertainty of this corrected temperature is within ±5 K at 900 K and smaller at lower temperatures. Details of the temperature correction method is provided in [25,26].

The sampled gas is transferred via a heated line at 473 K to a Horiba emission bench and a Shimadzu gas chromatography (GC) for species analysis. CO and CO_2 are measured by the Horiba emission bench using a non-dispersive infrared (NDIR) analyser, which has an accuracy of ±1% with a resolution of 20 ppm for CO and 30 ppm for CO_2. Sampled gases are also stored in heated storage loops and then analysed in the GC using a flame ionisation detector (FID). Liquid and gas standards are used in junction with the effective carbon number method [27,28] to convert the FID peak areas to species molar fractions. Details of the species analysis and calibration can be found in [29]. In this work, only the major intermediate species

that are well separated on the GC spectra are reported. A nominal 10% uncertainty is assumed for the GC analysis.

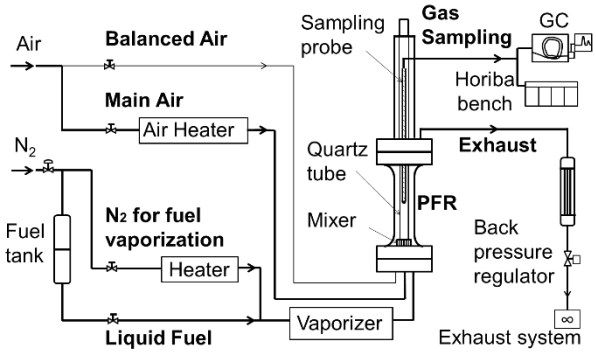

Figure 1 Schematic of the pressurised flow reactor system at the University of Melbourne

2.2. Experimental conditions

Table 1 shows the experimental conditions used in this work. Neat iso-octane (99.5%), ethanol (99.97%), and their mixtures are tested at 10 bar and two nominal reactor temperatures, 650 K and 875 K. The nominal temperature is measured at the location of the mixer (0 mm of the reactor length). A fixed air flow rate and equivalence ratio are used for all fuels tested. The fuel concentrations in the reactant mixture are similar to previous studies that used stoichiometric mixtures with nitrogen as the dilution gas [30,31]. The species sampling and gas temperature measurement are carried out downstream of the mixer from 5 to 905 mm. All experimental data are provided in the Supplementary Materials.

Table 1 Experimental conditions in the flow reactor for ethanol/iso-octane mixtures.

Fuel	Reactor temperature [b] (K)	Reactor pressure [c] (bar)	ϕ	Flow rate [d] (g/s)			Initial molar composition			
				Air	N_2	Fuel	C_2H_5OH (ppm)	IC_8H_{18} (ppm)	O_2 (%)	N_2 (%)

E0	650, 875	10.0	0.058	6.0	0.33	0.023	0	915	19.86	80.05
E10 [a]	650, 875	10.0	0.058	6.0	0.33	0.024	267	851	19.85	80.04
E20	650, 875	10.0	0.058	6.0	0.33	0.025	553	782	19.85	80.02
E50	650, 875	10.0	0.058	6.0	0.33	0.029	1540	544	19.83	79.96
E85	650, 875	10.0	0.058	6.0	0.33	0.035	3019	188	19.81	79.87
E100	650, 875	10.0	0.058	6.0	0.33	0.039	3802	0	19.80	79.82

[a] E10: 10 vol% ethanol and 90 vol% iso-octane. Same for the rest ethanol blends.
[b] Nominal reactor temperature measured at the mixer (0 mm reactor length).
[c] Reactor pressure variation ≤ 0.05 bar.
[d] Measurement uncertainty for the flow rate of air, N_2 and fuel is 2.7%, 5.5% and 0.5% respectively.

2.3. Kinetic simulation method

Kinetic simulation is performed using the Plug Flow Reactor model in Chemkin Pro [32]. The gasoline surrogate model by Mehl et al. [33] is used, which has been found to perform satisfactorily for ethanol and alkane mixtures [15,34]. The temperature profiles determined during the experiments are input to the simulation to solve species concentrations. The simulations are conducted with the origin at the location of the mixer and no profile shifting is applied.

3. Results and discussion

3.1. Impact of ethanol on oxidation of iso-octane at 650 K

Ethanol/iso-octane mixtures are first investigated at 650 K. At this temperature, oxidation of iso-octane is near the peak of its low temperature reactivity, as indicated by the variation of CO formation with temperature in Figure 2 [15].

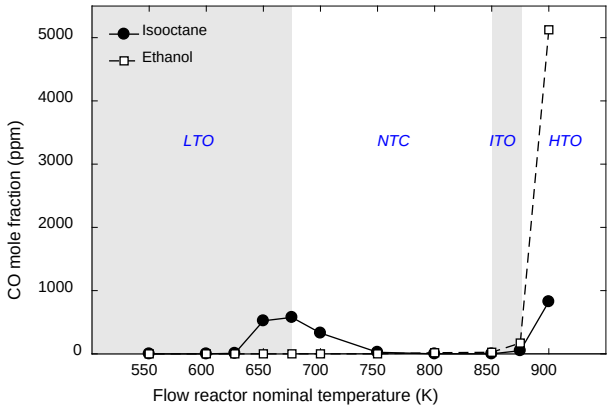

Figure 2 CO formation from iso-octane and ethanol in the flow reactor at 10 bar, ϕ = 0.058, τ = 0.21s, 550-900 K [15]. LTO, ITO, HTO, and NTC indicate the oxidation regimes at low, intermediate, high temperatures and of negative temperature coefficient.

Intermediate species are measured along the reactor for all the fuels listed in Table 1. Figure 3 shows the results for iso-octane (E0) at 650 K as an example, with the results for other fuels reported in the Appendix. At this temperature, in addition to CO and CO_2, iso-octane oxidation produces four hydrocarbons and three oxygenated compounds as the major intermediate species, which in order of decreasing concentration are acetone (CH_3COCH_3), iso-butene (iC_4H_8), methacrolein (iC_3H_5CHO), acetaldehyde (CH_3CHO), propene (C_3H_6), ethene (C_2H_4), and methane (CH_4). Formaldehyde is not detected due to lack of response on the FID. The kinetic simulation using the gasoline surrogate model of Mehl et al. [33] shows a reasonable reproduction of the experiment, particularly for the formation of hydrocarbons (except propene). The formation of these species can be explained by the established low temperature degenerate chain branching mechanism [35] (as shown in Figure 5 in Section 3.2) where the chemistry proceeds via formation of fuel peroxyl radicals (ROO), internal hydrogen abstraction (ROO => QOOH), and further reactions to produce alkyl ketohydroperoxides to trigger the chain branching sequence. Further analysis of intermediate species formation will not be pursued for iso-octane, given the interest of this work is in fuel mixtures, and as noted in the next section, the overall reaction framework of iso-octane oxidation is essentially unaffected by ethanol addition.

The oxidation of neat ethanol remains unreactive at 650 K, as shown in Figure A.6, where negligible ethanol consumption and intermediate species formation are detected.

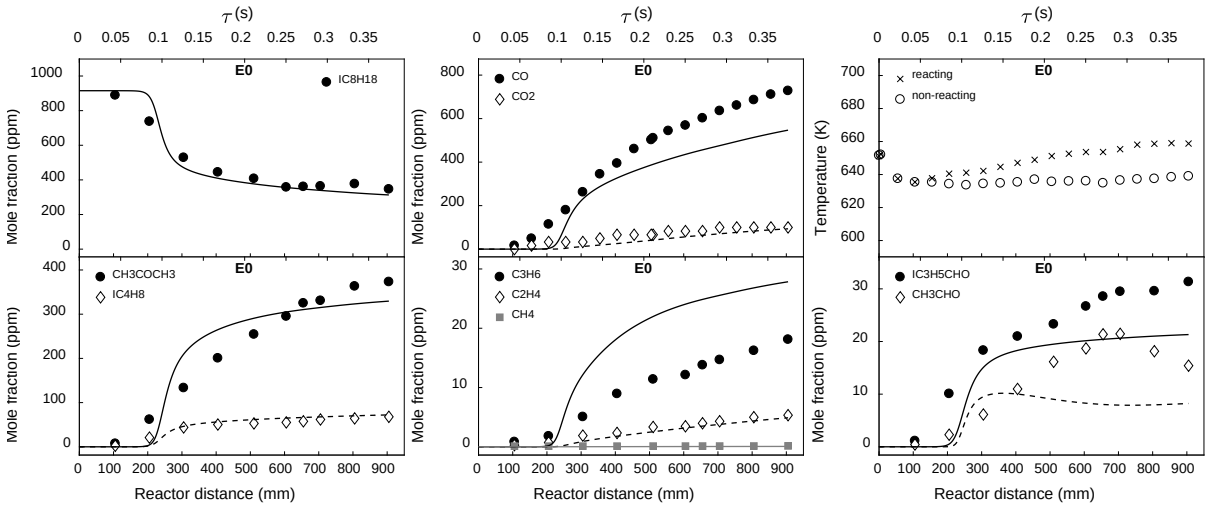

Figure 3 Time-history profiles of species concentration and temperature during iso-octane oxidation in the flow reactor at 650 K, 10 bar, ϕ = 0.058. Simulation uses the model by Mehl et al. [33]. Solid lines for filled symbols. Dashed lines for open symbols.

By choosing a constant residence time, the impact of ethanol blending on iso-octane oxidation can be demonstrated by intermediate species formation, as shown in Figure 4 for a residence time of 0.21 s (reactor distance ~ 510 mm). Similar results are obtained at other residence times except those closest to the mixer ($\leq$ 100 mm) when the fuel hardly reacts. It is evident that neat iso-octane is the most reactive fuel at this temperature and blending ethanol dramatically reduces the reactivity of the mixture. At 10% ethanol blending, the fuel conversion and the formation of intermediate species are nearly shut off. The reaction model of Mehl et al. [33] captures this non-linear blending behavior[1], although some discrepancies are observed in the E0 case. The model is therefore used to explore the kinetic details between ethanol and iso-octane in the rest of this paper.

[1] The simulation plots are generated by selecting the calculated species concentrations from each simulated species time history at the residence time and then plotting against the blending levels.

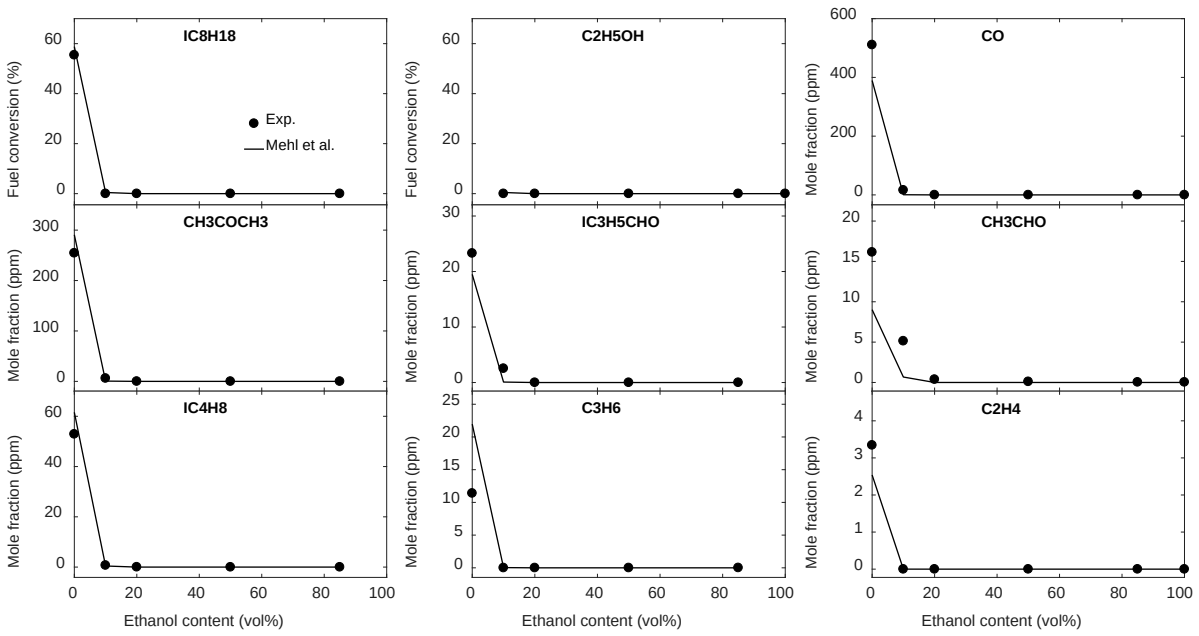

Figure 4 Fuel conversion and species formation as a function of ethanol content for ethanol/iso-octane mixtures in the flow reactor at 650 K, 10 bar, ϕ = 0.058 and τ = 0.21s (510 mm reactor distance). Simulation (lines) uses the model by Mehl et al. [33].

3.2. Analysis of ethanol/iso-octane interactions at 650 K

To understand the strong inhibiting effect of ethanol on iso-octane oxidation, reaction flux analysis is first carried out to the model of Mehl et al. [33] at a residence time of 0.087 s (reactor distance 208 mm). This corresponds to an iso-octane conversion of 5% in E0 and 0.024% in E10 in order to avoid kinetic ramifications at the later stage of the oxidation. The simulation results in Figure 5 indicate that adding 10 vol% ethanol barely changes the reaction flux distribution in iso-octane oxidation despite the substantial reduction in the overall reactivity. This is consistent with the finding of Dagaut and Togbe [22] that n-heptane/ethanol mixtures with different ethanol blend levels showed very similar oxidation paths.

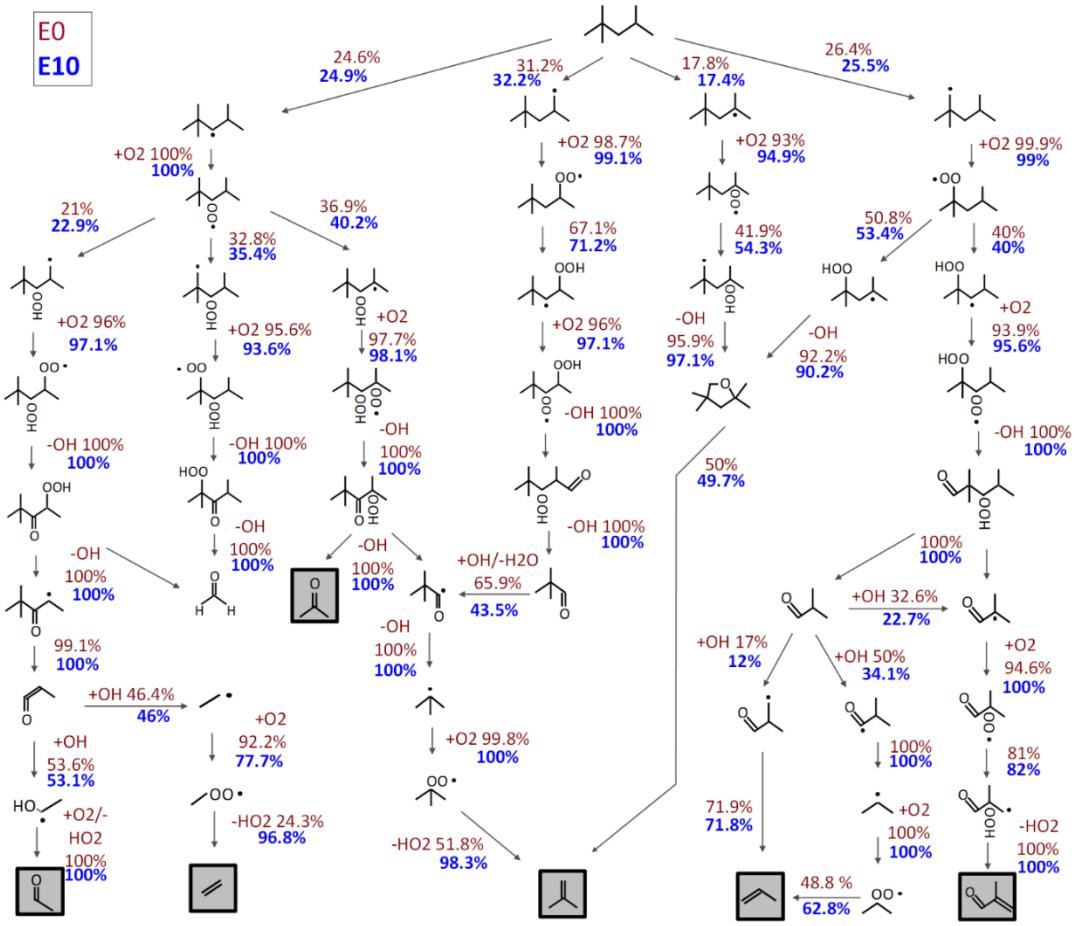

Figure 5 Major pathways for iso-octane oxidation in E0 (red) and E10 (blue) at 650 K, 10 bar, ϕ = 0.058 and τ = 0.087s. Iso-octane conversion is 5% in E0 and 0.024% in E10. The compounds in shaded boxes are major species measured in this work.

The weak impact of E10 on the reaction flux distribution suggests that subject to the kinetic model used here, the strong inhibiting effect of ethanol is not due to ethanol interfering with specific reaction pathways in iso-octane oxidation mechanism, but rather due to an overall impact on the entire reaction mechanism which takes effect from the start of the reaction, i.e. affecting the very first steps that convert the fuel molecule to fuel radicals and all subsequent reactions. Therefore, the impact of ethanol on fuel consumption is next investigated.

3.2.1. Effect of ethanol blending on fuel consumption rate

Figure 6 depicts the simulated consumption rates of iso-octane and ethanol as a function of ethanol content at a residence time of 0.087 s (corresponding to an iso-octane conversion of 5% in E0 and 0.024% in E10). With 10 vol.% ethanol added, the consumption rate of iso-octane is reduced by five orders of magnitude. This reduction is not due to the reduced initial

iso-octane concentration in the reactants, as evidenced by the dashed line in Figure 6 which shows reaction rates of neat iso-octane at the same concentrations as those in the ethanol/iso-octane mixtures.

Figure 6 also shows that the reaction rate of ethanol consumption falls similarly to iso-octane with increased ethanol content, which further confirms that the reaction rate is not controlled by the initial fuel concentration and other factors must be in play.

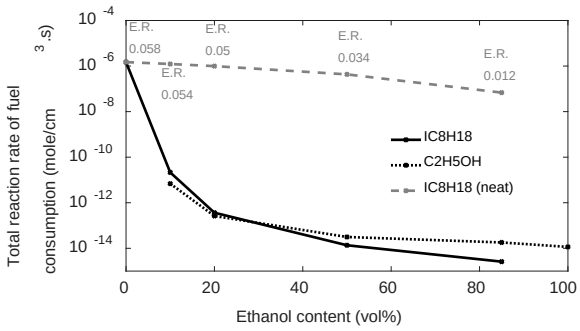

Figure 6 Simulated fuel consumption rate as a function of ethanol content at 650 K, 10 bar, ϕ = 0.058 and τ = 0.087s (208 mm reactor distance). The dashed line denotes simulations of iso-octane/air mixtures with the same iso-octane concentration as that in the iso-octane/ethanol/air mixtures.

3.2.2. Effect of ethanol blending on radicals consuming fuels

The next step is to investigate how iso-octane and ethanol are consumed. Figure 7 shows the reaction pathways that consume the iso-octane and ethanol at different ethanol blending levels at the fixed residence time of 0.087 s. Almost all iso-octane is consumed by reactions with OH, HO_2 radicals and O_2 to form iso-octyl radicals. Similarly, more than 90% of the ethanol, irrespective of the blending levels, is also consumed by OH, HO_2 radicals and O_2 to form C_2H_5O isomer radicals.

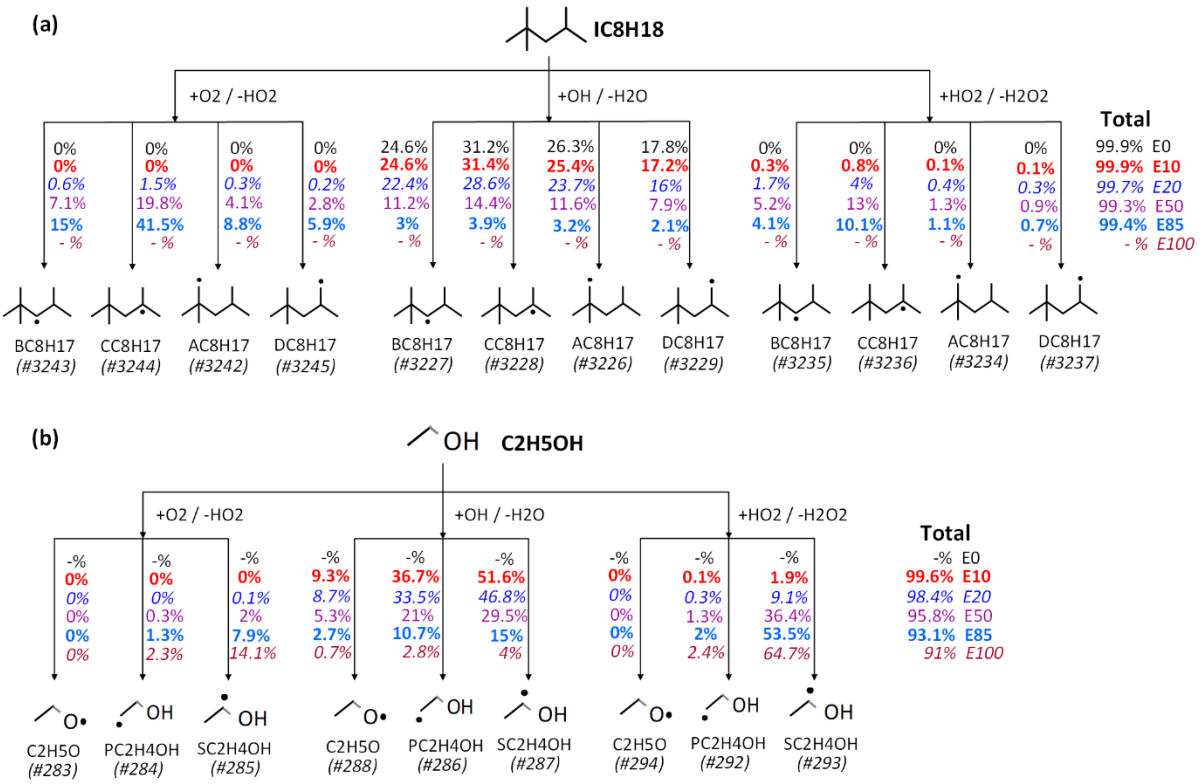

Figure 7 Reaction pathways consuming iso-octane (a) and ethanol (b) during the oxidation of E0 to E100 ethanol/iso-octane mixtures at 650 K, 10 bar, ϕ = 0.058 and τ = 0.087s (208 mm reactor distance).

Figure 8(a) shows the contribution of OH, HO_2 radicals and O_2 to the consumption of iso-octane at different ethanol blending levels. The OH radical dominates the consumption of iso-octane in E50 and lower blends, whereas O_2 becomes more important at higher ethanol contents (e.g. E85). The HO_2 radical is overall less important. Similar results are obtained for ethanol in Figure 8(b) where the OH radical dominates ethanol consumption at lower ethanol contents. However, the HO_2 radical, instead of O_2, becomes more important at higher ethanol contents.

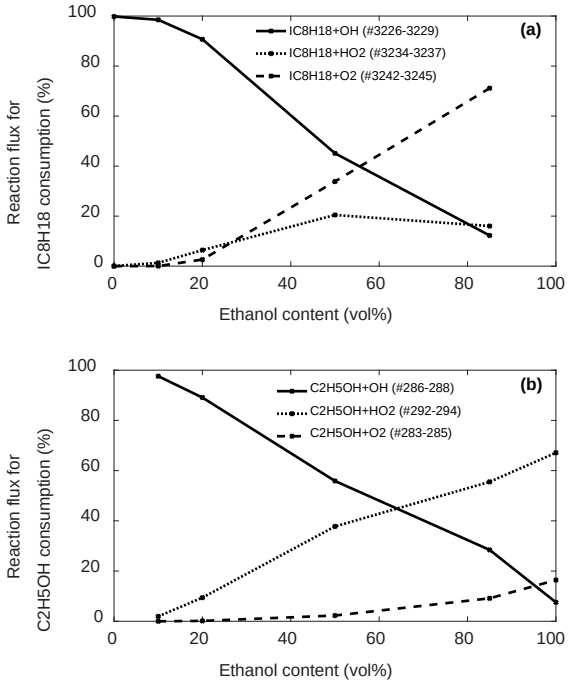

Figure 8 Relative contribution of OH, HO_2, and O_2 to the consumption of a) iso-octane and b) ethanol at varying ethanol content at 650 K, 10 bar, ϕ = 0.058 and τ = 0.087s.

The results in Figure 8 should be understood in the context that the mixtures with ethanol content higher than 20 vol% barely react at the flow reactor conditions (Figure 4). Considering the dramatic change from E0 to E10 where the fuel consumption is dominated by OH radicals, further analysis is focused on the impact of ethanol on OH formation.

3.2.3. Imbalance of OH production/consumption with ethanol blending

Figure 9 shows the mole fraction of OH radicals versus ethanol content at 650 K. Consistent with the fuel conversion (Figure 4), adding 10% ethanol substantially suppresses the OH production rate and therefore the OH molar fraction in the mixture.

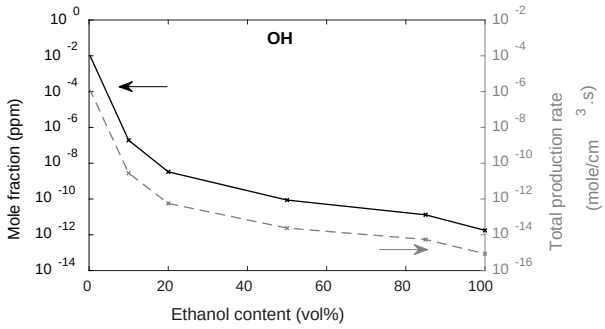

Figure 9 Simulated OH concentration and production rate as a function of ethanol content at 650 K, 10 bar, $\phi = 0.058$ and $\tau = 0.087$s.

Further analyses are conducted to the reaction paths that produce and consume OH radicals. As shown in Figure 10, for neat iso-octane (E0), OH radicals are produced primarily by the decomposition of C_8 species, including hydroperoxyl radicals, peroxyl-hydroperoxyl radicals, and ketohydroperoxides. The produced OH radicals are nearly all consumed by iso-octane to form iso-octyl radicals that then undergo O_2 addition and internal isomerization to regenerate the C_8 peroxyl species. This process builds a surplus of OH, of order 0.01 ppm, in the reaction mixture at 0.087s (Figure 9) which sustains the oxidation of iso-octane at this condition.

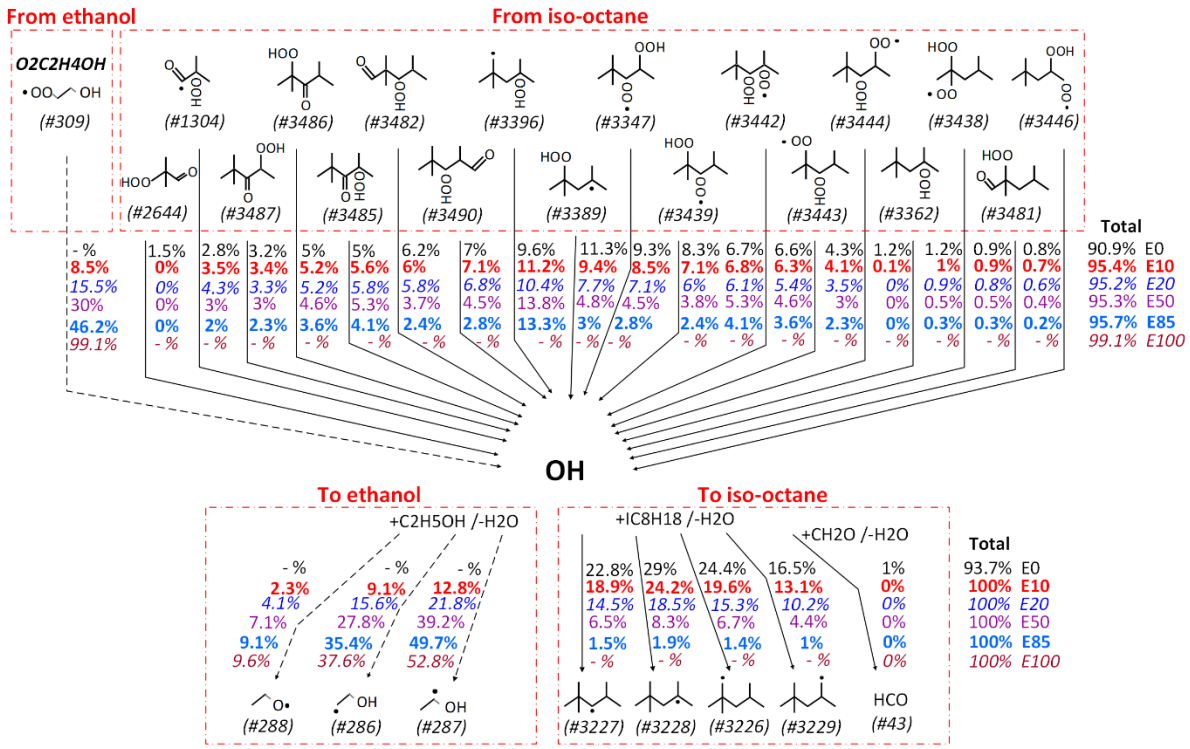

Figure 10 Major reaction pathways for OH radical production (top) and consumption (bottom) in oxidation of ethanol/iso-octane mixtures at 650 K, 10 bar, ϕ = 0.058 and τ = 0.087s. Dashed lines correspond to ethanol-related reactions.

Addition of ethanol affects both the production and consumption of OH radicals. Ethanol can form three fuel radicals, pC_2H_4OH (), sC_2H_4OH () and C_2H_5O (), which for E10 are nearly all from reactions with OH radical (Figure 7).

The sC_2H_4OH radical accounts for over 50% of the consumed ethanol in E10 and reacts exclusively (100%) with O_2 to form acetaldehyde (CH_3CHO) and HO_2, as shown in Reaction 1.

$$sC_2H_4OH + O_2 \rightleftharpoons CH_3CHO + HO_2 \qquad \text{(R1)}$$

The C_2H_5O radical accounts for approximately 10% of the reacted ethanol in E10, which mostly (90.6%) undergoes β-scission to produce formaldehyde (CH_2O) and CH_3 by Reaction 2, whereas the rest reacts to produce CH_3CHO via Reaction 3 (6%) and Reaction 4 (3.4%). The resultant CH_3CHO, CH_2O and HO_2 species are relatively stable at the condition and provide negligible contribution to the overall chain propagation. CH_3 and H radicals are more reactive

but their contribution to the overall chain propagation is small due to the small fraction of C_2H_5O radical in the mixture.

$$C_2H_5O \rightleftharpoons CH_2O + CH_3 \quad (90.6\%) \quad (R2)$$

$$C_2H_5O \rightleftharpoons CH_3CHO + H \quad (6\%) \quad (R3)$$

$$C_2H_5O + O_2 \rightleftharpoons CH_3CHO + HO_2 \quad (3.4\%) \quad (R4)$$

The third ethanol radical, pC_2H_4OH, accounts for roughly 40% of ethanol consumed in E10, of which nearly all (99.9%) undergoes O_2 addition to produce an $O_2C_2H_4OH$ (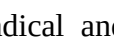) radical and then decomposes (100%) to produce an OH radical and two formaldehydes (CH_2O), as shown in Reactions 5 and 6. Decomposition of $O_2C_2H_4OH$ radical is therefore the only major channel to produce OH radicals from ethanol oxidation. Direct decomposition of pC_2H_4OH to C_2H_4 and OH does not take place at this condition.

$$pC_2H_4OH + O_2 \rightleftharpoons O_2C_2H_4OH \quad (R5)$$

$$O_2C_2H_4OH \rightarrow OH + CH_2O + CH_2O \quad (R6)$$

Combining the production and consumption of OH, the ethanol oxidation contributes to approximately 8.5% of the total OH production and consumes 24.2% of the total OH in the mixture[2]. A deficit in the OH budget therefore results in the oxidation of E10 and higher blends (Figure 10).

Since this result is obtained at a particular moment (0.087s) in the reaction, temporal analysis is further conducted for the evolution of the OH production/consumption ratio along the reactor. As shown in Figure 11, the ratio starts at roughly 0.1 and rapidly increases to approximately 0.35 at around 25 mm and remains roughly constant thereafter. The imbalanced OH production/consumption ratio exerts a cumulative impact on the E10 oxidation, where fewer OH radicals lead to a reduced consumption of iso-octane and subsequently even less OH radicals are produced for the next round of reaction. This process continues as the reaction progresses and the ‘snowballing’ effect eventually reduces the OH concentration by orders of magnitude compared with the neat iso-octane case.

[2] The 24.2% of OH consumption matches the 23.9 mol.% of ethanol in E10, which is consistent with the non-selective nature of OH attack on fuel molecules.

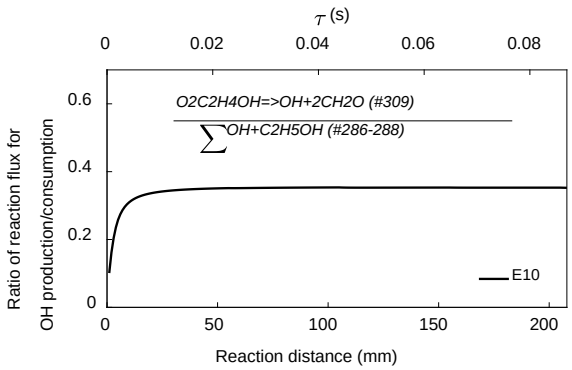

Figure 11 Ratio of OH production/consumption from ethanol oxidation in E10 as a function of reactor distance at 650 K, 10 bar, ϕ = 0.058.

Figure 12 demonstrates the snow-ball effect by plotting the net production rate of OH vs. ethanol blending levels at different reaction time. Near the very start of the oxidation (1 – 5 mm) where the imbalanced OH production/consumption has occurred but not yet produced significant impact, a roughly linear relation occurs between the OH production and ethanol contents despite even smaller OH production/consumption ratios than at the later stage (e.g. Figure 11 for E10). As the reaction progresses, the deficit in OH production accumulates and results in an increasingly slow OH production rate relative to neat iso-octane. Eventually a strongly non-linear blending behavior is established on OH production as shown in Figure 9.

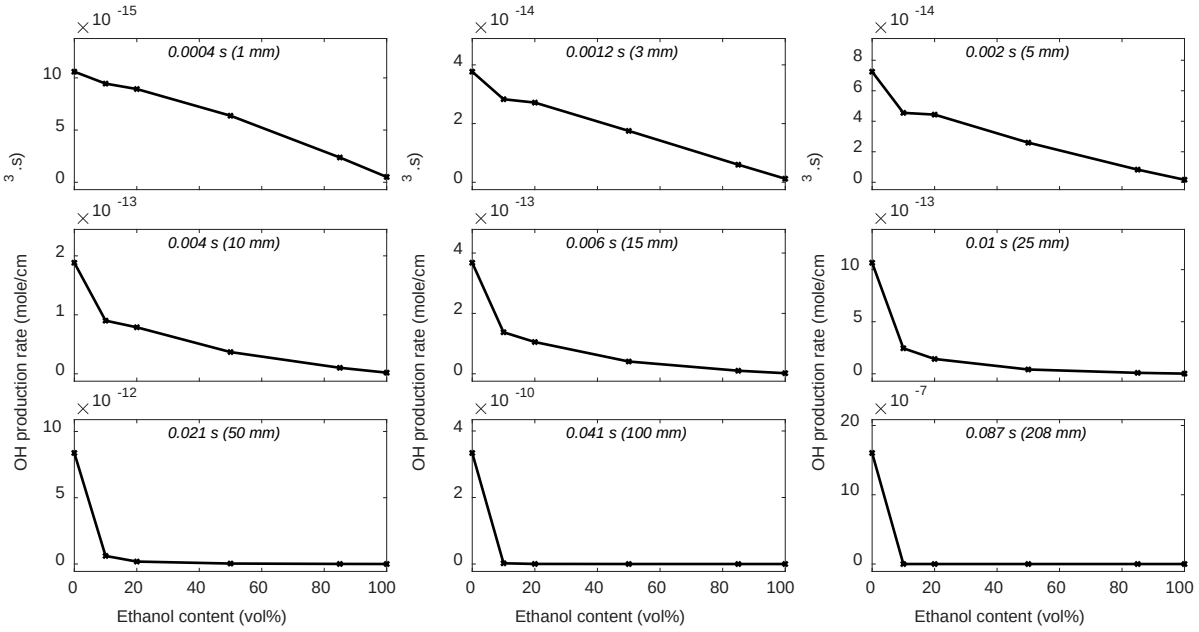

Figure 12 Simulated net production rate of OH radicals in ethanol/iso-octane mixtures as a function of ethanol content at varied residence times (reactor distance) at 650 K, 10 bar, ϕ = 0.058.

It should be noted that this OH depleting effect can take place in an environment where the absolute OH production rate in fact increase with time. As shown in Figure 13, the net OH production rate of E0 increases significantly along the reactor (up to 240 mm) due to the active low temperature oxidation of iso-octane. The OH production rate also increases for E10; however, due to the OH-depleting effect discussed above, such an increase is drastically reduced at any given moment. At 0.087 s, the OH production rate is hundreds of thousand times lower for E10 than for E0, which substantially slows the oxidation process.

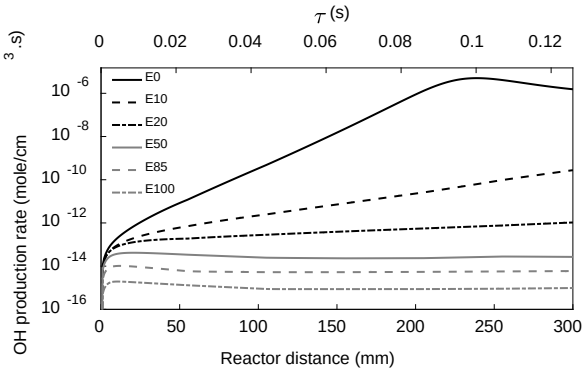

Figure 13 Net production rate of OH radicals in ethanol/iso-octane mixtures as a function of reactor distance at 650 K, 10 bar, ϕ = 0.058.

3.3. Impact of ethanol on oxidation of iso-octane at 875 K

The oxidation of ethanol/iso-octane mixtures in the intermediate temperature regime is now studied. Figure 14 and Figure 15 show the species time-history for the oxidation of neat iso-octane (E0) and neat ethanol (E100) at 875 K. The results for the mixtures (E10, E20, E50 and E85) are provided in the Appendix. For iso-octane, eight hydrocarbons and three oxygenated compounds are measured as the oxidation intermediates, which in the order of decreasing concentration are iso-butene (iC_4H_8), acetone (CH_3COCH_3), propene (C_3H_6), methacrylaldehyde (iC_3H_5CHO), 2,4,-dimethyl-2-pentene ($y\text{-}C_7H_{14}$), 4,4-dimethyl-2-pentene ($o\text{-}C_7H_{14}$), 2,4,-dimethyl-1-pentene ($x\text{-}C_7H_{14}$), 4,4-dimethyl-1-pentene ($p\text{-}C_7H_{14}$), acetaldehyde (CH_3CHO), methane (CH_4) and ethylene (C_2H_4). This is consistent with the findings in other experiments [19,30,36–38] and also similar to the results at 900 K in the same reactor [34]. In contrast to the peroxyl chemistry at low temperatures, iso-octane oxidation at this temperature is mainly via β-scission of iso-octyl radicals to produce olefins such as the detected iso-butene and C7 olefins. For neat ethanol, three intermediates are detected, acetaldehyde (CH_3CHO), ethylene (C_2H_4) and methane (CH_4), with acetaldehyde being the most abundant intermediate species. This result is also consistent with observations of ethanol oxidation in other reactors, e.g. [31,39,40].

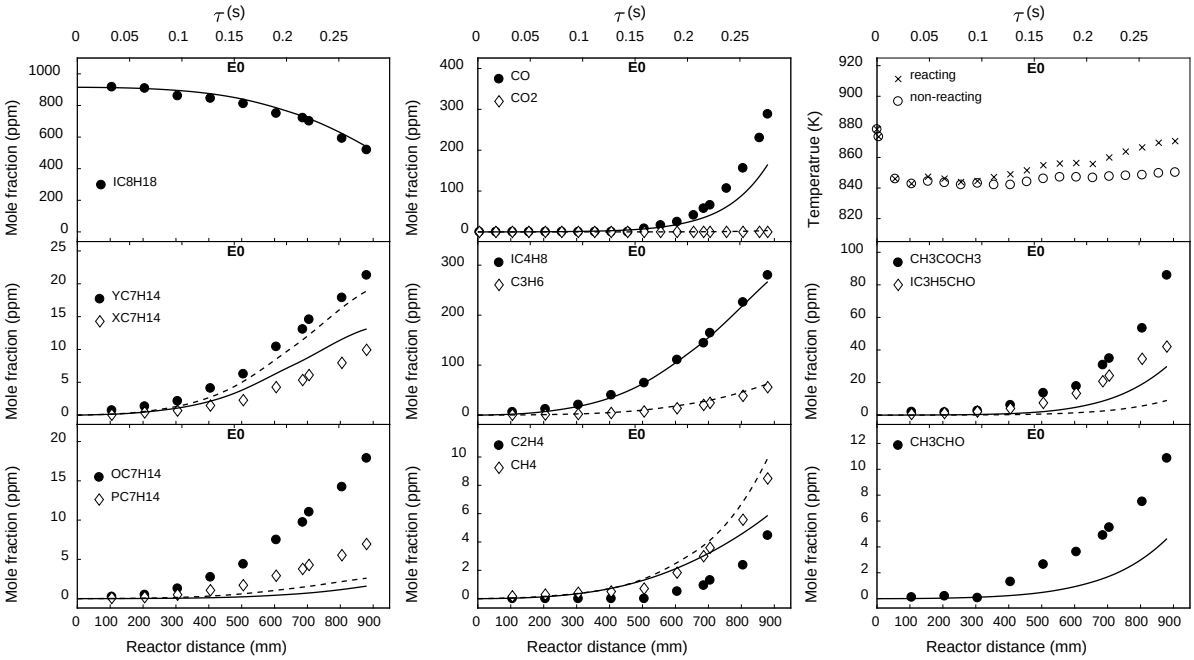

Figure 12 Time-history profiles of species concentration and temperature during iso-octane oxidation in the flow reactor at 875 K, 10 bar, ϕ = 0.058. Simulation uses the model by Mehl et al. [33]. Solid lines for filled symbols. Dashed lines for open symbols.

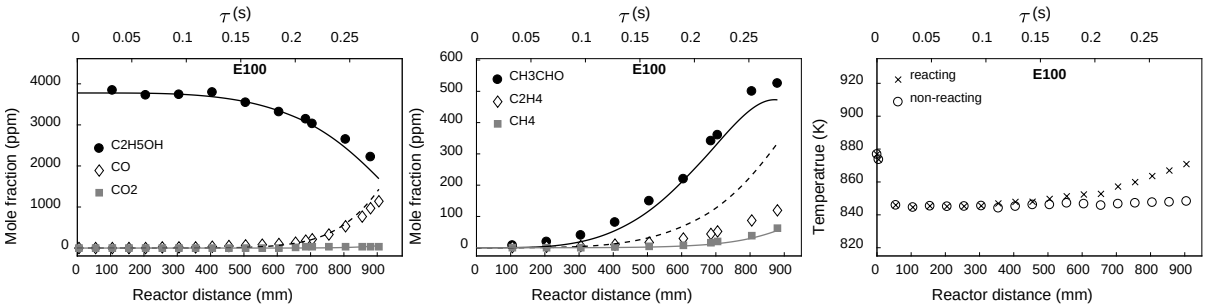

Figure 13 Time-history profiles of species concentration and temperature during ethanol oxidation in the flow reactor at 875 K, 10 bar, ϕ = 0.058. Simulation uses the model by Mehl et al. [33]. Solid lines for filled symbols. Dashed lines for open symbols.

With a residence time of 0.21 s (corresponding to a reactor distance of approximately 685 mm), the fuel conversion and species formation are shown in Figure 16 as a function of ethanol content. Results at other residence times are also similar. A significantly different blending behavior than that at 650 K is observed. The similar fuel conversion percentages across the blending range from E0 to E100 indicate that the two fuels are of similar reactivity and react independently at the condition. This weak interactions between iso-octane and

ethanol are also reflected by the formation of intermediate species which can be categorized into three groups:

(i) species exclusively from the oxidation of iso-octane, including iso-butene (iC_4H_8), propene (C_3H_6), acetone (CH_3COCH_3), C_7 olefins (y-, x-, o-, p-C_7H_{14}), and methacrolein (iC_3H_5CHO);

(ii) species mostly from the oxidation of ethanol, including acetaldehyde (CH_3CHO) and ethene (C_2H_4);

(iii) species from the oxidation of both fuels, including CO and methane (CH_4).

For the first two groups, a roughly linear relation can be approximated between the species concentrations and the respective content of iso-octane or ethanol. For example, the concentration of iso-butene decreases approximately linearly with the reduced iso-octane content, from roughly 150 ppm in E0 to 30 ppm in E85. Similarly, the concentration of acetaldehyde, which is predominantly formed by ethanol (approximately 100 times more than for iso-octane), increases approximately linearly with ethanol content. The almost linear variation again suggests that both fuels react largely independently. The formation of CO and methane shows a weak dependence on ethanol content since ethanol produces more of these species at this temperature; therefore, the two fuels contribute to the common products based on their contents in the reactant.

Kinetic simulation using the gasoline surrogate model by Mehl et al. [33] captures this blending behaviour reasonably, particularly for the major species including the two fuel compounds, iso-butene, acetaldehyde and CO. More significant discrepancies are observed for C_7 olefines and C_3-C_4 oxygenates with iso-octane, and for ethene with ethanol, which are consistent with the results at 900 K [34]. Overall, both the experiment and model suggest that the impact of ethanol on the intermediate-temperature oxidation of iso-octane is weak. A similar conclusion was drawn by Barraza-Botet and Wooldridge from their RCM study at 930 K and 10 bar [16].

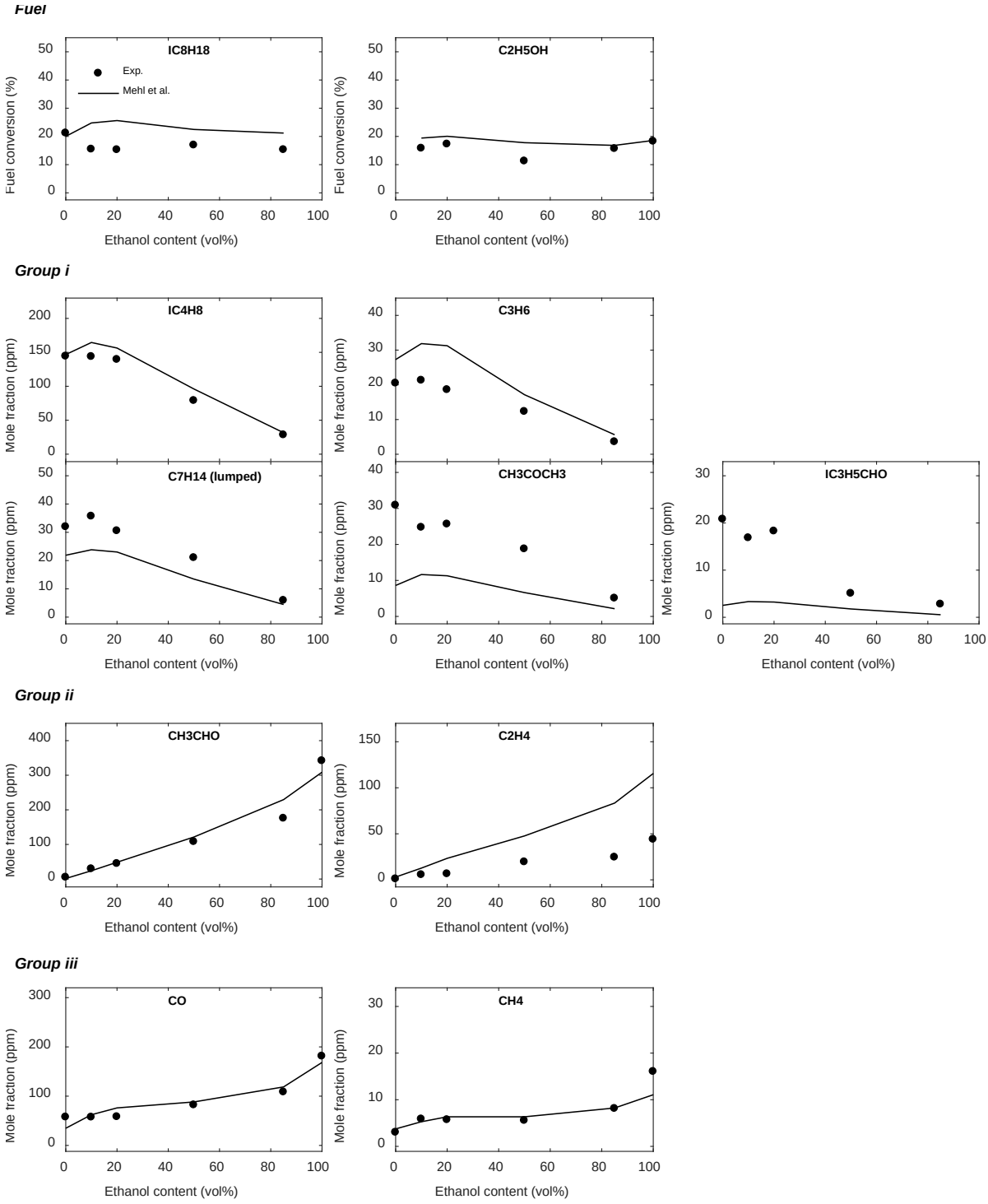

Figure 14 Species formations as a function of ethanol content for ethanol/iso-octane mixtures in the flow reactor at 875 K, 10 bar, ϕ = 0.058 and τ = 0.21s (685 mm reactor distance). Simulation (lines) uses the reaction model by Mehl et al. [33].

In summarizing the above analysis, a common working mechanism can be used to explain the differing ethanol/iso-octane interactions at low and intermediate temperatures. That is, each fuel component reacts by following its own mechanism, and they interact mainly via

the shared radical pool, with the cross reactions of large fuel-like radicals playing at most a secondary role. The different blending behaviours are attributed to each component's specific capability to feed and drain the radical pool during the reaction. For example, at low temperatures, the ethanol oxidation consumes OH radicals according to the ethanol content in the mixture but is unable to feed the radical pool with the corresponding amount of OH. As shown in Figure 10, for E10 oxidation at 650 K, the ethanol oxidation contributes 8.5% of total OH production but consumes 24.2% of total OH when 5% iso-octane is reacted. The deficiency in OH budget drains the radical pool and slows down the oxidation of the mixture. On the other hand, ethanol oxidation appears to be more self-sufficient at intermediate temperatures. Reaction flux analysis conducted to E10 at 875 K shows that, at 5% iso-octane consumption (378 mm reactor distance), the ethanol oxidation contributes to 18.8% of total OH production and consumes 19.5% of total OH. The two fuel components therefore appear to react independently to produce a linear blending. A concept of self-sufficiency can therefore be introduced to describe the impact of fuel blending on mixture reactivity, with a self-sufficiency index (SSI) defined as

$$SSI = \frac{contribution\,(\%)\,to\ production\,of\ \ primary\ \ fuel\text{-}consuming\ species}{contribution\,(\%)\,to\,consumption\,of\ \ primary\ \ fuel\text{-}consuming\ species}$$

where the SSI is between 0 and 1 for the less reactive component in a mixture. An SSI < 1 (e.g. 0.35 for ethanol in E10 oxidation at 650 K) means that the component's oxidation is deficient in regenerating active radicals and tends to deplete the radical pool and cause inhibiting effect. An SSI close to 1 (e.g. 0.96 for ethanol in E10 oxidation at 875 K) means that the component's oxidation is self-sufficient, and a linear blending is expected when this applies to all components in a mixture. The evaluation of SSI should be conducted at an early stage of oxidation where the system is dominated by fuel consumption without significant oxidation of intermediate species. The primary fuel-consuming species in most cases should be OH, whereas HO_2 and O_2 could also be important in low reactivity mixtures. The concept is expected to be particularly useful for mixtures consisting of fuel components of comparable reactivities, such as for ethanol/iso-octane/toluene mixtures, where SSI can help to explain the blending effects. For mixtures made of components of very different reactivities, e.g. n-heptane/ethanol, the reactivity will be dominated by the high reactivity component and the other component will always show an inhibiting effect. Further development of the concept will be subject to future work.

3.4. Comments on further model development

The observed impacts of ethanol on the oxidation of iso-octane in this paper suggest explanations for the recently reported octane blending behaviour of these two compounds [15]. In particular, the observed, strong inhibition effect of ethanol at low temperatures can be related to the synergistic blending where ethanol enhances the anti-knock performance of iso-octane in an octane rating engine. Since engine autoignition occurs over a range of temperatures, the octane blending behaviour should rely more on the non-linear interactions between these two fuels at low temperatures rather than the roughly linear interactions at intermediate temperatures.

More quantitative account of the chemistry responsible for engine autoignition behaviours will require coupling of a chemical kinetic model with a physical model that describes the evolution of cylinder conditions, such as the two-zone model in our recent work [41]. Furthermore, due to the differing thermochemical conditions in engines and more fundamental reactors, chemical kinetic models also need to be developed in several aspects, as discussed below

- High pressure data are required for model validation. Most existing data for the oxidation of ethanol/iso-octane mixtures were obtained at 10 atm. or lower pressures. Ignition delays and species concentrations at higher pressures, up to and even exceeding 40 bar, are needed to develop and validate models for use in engines.

- Combustion products commonly exist in the unburned charge of firing engines since some of the exhaust gases are always recirculated in one way or another. These gases, particularly nitric oxide (NO), can significantly affect autoignition. The residual gas chemistry therefore should be an integral part of combustion chemistry models.

- The transient conditions inside an engine cylinder are obviously different from the steady or quasi-steady processes in more fundamental experiments. The impact of such differences is generally unknown because it cannot be tested easily. Standard engines, such as the octane rating engine, with carefully calibrated initial and boundary conditions provide a potential means for studying such effects.

4. Conclusions

This work investigated the chemical interactions of iso-octane and ethanol in a flow reactor at 650 K and 875K, 10 bar and an equivalence ratio of 0.058. Kinetic simulation of the flow reactor at these conditions was conducted using the gasoline surrogate model by Mehl et al. [33]. The conclusions of this work are as follows.

- In the low temperature regime (650 K), the addition of 10 vol% ethanol to iso-octane dramatically suppressed iso-octane's low temperature reactivity and the formation of intermediate species, and further addition of ethanol effectively terminated the reaction.

- Kinetic modelling at 650 K found that the addition of 10 vol% ethanol had a negligible impact on the reaction flux distribution of iso-octane's oxidation, but rather slowed down iso-octane's entire chemistry due to a lack of OH radicals in the mixture. This lack of OH radicals, resulting from ethanol oxidation consuming more OH than it produced, was particularly prominent once the reaction was well established, and produced a disproportionate inhibiting effect on reactivity even at low ethanol content.

- In the intermediate temperature regime (875 K), iso-octane and ethanol demonstrated comparable oxidation reactivity. The fuel conversion and formation of intermediate species correlated roughly linearly with these fuels' concentrations in the reactant mixtures, indicating negligible interaction between the two compounds at these temperatures.

- These differing ethanol/iso-octane interactions could be explained by ethanol's varying capabilities to feed and drain the shared radical pool while each fuel component reacts within its own framework. In particular, ethanol was considered as a net "taker" and deficient in refilling the radical pool at low temperatures but became increasingly self-sufficient at intermediate temperatures. A self-sufficiency index was proposed to characterize the impact of fuel blending on mixture reactivity.

Given these results, the previously published synergistic (i.e. super-linear) octane blending of iso-octane and ethanol [1] appears to be the result of ethanol's scavenging of OH radicals at low temperatures, thereby suppressing iso-octane reactivity strongly. Further investigation in

a dynamic and more complex premixture environment that more closely resembles that of an operating engine is required to demonstrate this categorically.

Acknowledgements

This project is supported by the University of Melbourne and the Australian Research Council (DP140100846).

References

[1] T.M. Foong, K.J. Morganti, M.J. Brear, G. da Silva, Y. Yang, F.L. Dryer, The octane numbers of ethanol blended with gasoline and its surrogates, Fuel. 115 (2014) 727–739.
[2] T.G. Leone, E.D. Olin, J.E. Anderson, H.H. Jung, M.H. Shelby, R.A. Stein, Effects of Fuel Octane Rating and Ethanol Content on Knock, Fuel Economy, and CO2 for a Turbocharged DI Engine, SAE International Journal of Fuels and Lubricants. 7 (2014) 9–28.
[3] M. Storch, F. Hinrichsen, M. Wensing, S. Will, L. Zigan, The effect of ethanol blending on mixture formation, combustion and soot emission studied in an optical DISI engine, Applied Energy. 156 (2015) 783–792.
[4] J.E. Anderson, D.M. DiCicco, J.M. Ginder, U. Kramer, T.G. Leone, H.E. Raney-Pablo, T.J. Wallington, High octane number ethanol–gasoline blends: Quantifying the potential benefits in the United States, Fuel. 97 (2012) 585–594.
[5] R.A. Stein, D. Polovina, K. Roth, M. Foster, M. Lynskey, T. Whiting, J.E. Anderson, M.H. Shelby, T.G. Leone, S. VanderGriend, Effect of Heat of Vaporization, Chemical Octane, and Sensitivity on Knock Limit for Ethanol - Gasoline Blends, SAE International Journal of Fuels and Lubricants. 5 (2012) 823–843.
[6] J.E. Anderson, T.G. Leone, M.H. Shelby, T.J. Wallington, J.J. Bizub, M. Foster, M.G. Lynskey, D. Polovina, Octane Numbers of Ethanol-Gasoline Blends: Measurements and Novel Estimation Method from Molar Composition, SAE Technical Paper. (2012) Paper No. 2012-01-1274. doi:10.4271/2012-01-1274.
[7] I. Hunwartzen, Modification of CFR Test Engine Unit to Determine Octane Numbers of Pure Alcohols and Gasoline-Alcohol Blends, SAE Technical Paper. (1982) Paper No. 922325.
[8] M. Waqas, N. Naser, M. Sarathy, K. Morganti, K. Al-Qurashi, B. Johansson, Blending Octane Number of Ethanol in HCCI, SI and CI Combustion Modes, SAE International Journal of Fuels and Lubricants. 9 (2016) 659–682.
[9] N. Rankovic, G. Bourhis, M. Loos, R. Dauphin, Understanding octane number evolution for enabling alternative low RON refinery streams and octane boosters as transportation fuels, Fuel. 150 (2015) 41–47.
[10] T.M. Foong, K.J. Morganti, M.J. Brear, G. da Silva, Y. Yang, F.L. Dryer, The Effect of Charge Cooling on the RON of Ethanol/Gasoline Blends, SAE Int. J. Fuels Lubr. 6 (2013) 34–43.

[11] ASTM International, Standard test method for motor octane number of spark-ignition engine fuel, ASTM D2700-11, 2011.
[12] ASTM International, Standard test method for research octane number of spark-ignition engine fuel, ASTM D2699-11, 2011.
[13] H. Song, H.H. Song, Ignition delay measurements of iso-octane/ethanol blend fuel in a rapid compression machine, in: Proceedings of the European Combustion Meeting 2015, Budapest, 2015: pp. 1–6.
[14] G.E. Bogin, J. Luecke, M.A. Ratcliff, E. Osecky, B.T. Zigler, Effects of iso-octane/ethanol blend ratios on the observance of negative temperature coefficient behavior within the Ignition Quality Tester, Fuel. 186 (2016) 82–90.
[15] Z. Lu, Y. Yang, M.J. Brear, Oxidation of PRFs and ethanol/iso-octane mixtures in a flow reactor and the implication for their octane blending, Proceedings of the Combustion Institute. 37 (2019) 649–656.
[16] C.L. Barraza-Botet, M.S. Wooldridge, Combustion chemistry of iso-octane/ethanol blends: Effects on ignition and reaction pathways, Combustion and Flame. 188 (2018) 324–336.
[17] M. Yahyaoui, O. Mathieu, C. Dotoum, N. Chaumeix, C.-E. Paillard, Autoignition of a gasoline surrogate containing various blend ratios of ethanol: shock tube experiments and detailed kinetic modeling, in: Mediterranean Combustion Symposium, Italy, 2011.
[18] P. Saisirirat, C. Togbé, S. Chanchaona, F. Foucher, C. Mounaim-Rousselle, P. Dagaut, Auto-ignition and combustion characteristics in HCCI and JSR using 1-butanol/n-heptane and ethanol/n-heptane blends, Proceedings of the Combustion Institute. 33 (2011) 3007–3014.
[19] F.M. Haas, M. Chaos, F.L. Dryer, Low and intermediate temperature oxidation of ethanol and ethanol–PRF blends: An experimental and modeling study, Combustion and Flame. 156 (2009) 2346–2350.
[20] D. Vuilleumier, D. Kozarac, M. Mehl, S. Saxena, W.J. Pitz, R.W. Dibble, J.-Y. Chen, S. Mani Sarathy, Intermediate temperature heat release in an HCCI engine fueled by ethanol/n-heptane mixtures: An experimental and modeling study, Combustion and Flame. 161 (2014) 680–695.
[21] E. Singh, E.-Al. Tingas, D. Goussis, H.G. Im, S.M. Sarathy, Chemical Ignition Characteristics of Ethanol Blending with Primary Reference Fuels, Energy Fuels. (2019).
[22] P. Dagaut, C. Togbé, Experimental and modeling study of the kinetics of oxidation of ethanol-n-heptane mixtures in a jet-stirred reactor, Fuel. 89 (2010) 280–286.
[23] Q. Fan, Z. Wang, Y. Qi, Y. Wang, Investigating auto-ignition behavior of n-heptane/iso-octane/ethanol mixtures for gasoline surrogates through rapid compression machine measurement and chemical kinetics analysis, Fuel. 241 (2019) 1095–1108.
[24] F.L. Dryer, F.M. Haas, J. Santner, T.I. Farouk, M. Chaos, Interpreting chemical kinetics from complex reaction–advection–diffusion systems: Modeling of flow reactors and related experiments, Progress in Energy and Combustion Science. 44 (2014) 19–39.
[25] Z. Lu, J. Cochet, N. Leplat, Y. Yang, M.J. Brear, A High-Pressure Plug Flow Reactor for Combustion Chemistry Investigations, Meas. Sci. Technol. 28 (2017) 105902.
[26] Z. Lu, Investigation of autoignition chemistry of ethanol and primary reference fuels in a pressurised flow reactor, Ph.D., University of Melbourne, 2018.
[27] J.T. Scanlon, D.E. Willis, Calculation of Flame Ionization Detector Relative Response Factors Using the Effective Carbon Number Concept, J Chromatogr Sci. 23 (1985) 333–340.
[28] A.D. Jorgensen, K.C. Picel, V.C. Stamoudis, Prediction of gas chromatography flame ionization detector response factors from molecular structures, Anal. Chem. 62 (1990) 683–689.

[29] H. Yuan, Octane blending and oxidation chemistry of ethanol-hydrocarbon mixtures, Ph.D., University of Melbourne, 2017.
[30] F.L. Dryer, K. Brezinsky, A Flow Reactor Study of the Oxidation of n-Octane and Iso-Octane, Combustion Science and Technology. 45 (1986) 199–212.
[31] J. Li, A. Kazakov, M. Chaos, F.L. Dryer, Chemical Kinetics of Ethanol Oxidation, in: 5th US Combustion Meeting, The Combustion Institute, San Diego, 2007.
[32] CHEMKIN-PRO 15131, Reaction Design: San Diego, 2013.
[33] M. Mehl, W.J. Pitz, C.K. Westbrook, H.J. Curran, Kinetic modeling of gasoline surrogate components and mixtures under engine conditions, Proceedings of the Combustion Institute. 33 (2011) 193–200.
[34] H. Yuan, Z. Lu, Z. Chen, Y. Yang, M.J. Brear, J.E. Anderson, T. Leone, Oxidation of ethanol and hydrocarbon mixtures in a pressurised flow reactor, Combustion and Flame. 199 (2019) 96–113.
[35] H.J. Curran, P. Gaffuri, W.J. Pitz, C.K. Westbrook, A comprehensive modeling study of iso-octane oxidation, Combustion and Flame. 129 (2002) 253–280.
[36] P. Dagaut, M. Reuillon, M. Cathonnet, High Pressure Oxidation of Liquid Fuels From Low to High Temperature. 1. n-Heptane and iso-Octane., Combustion Science and Technology. 95 (1993) 233–260.
[37] J.-S. Chen, The oxidation of iso-octane at elevated pressures, Ph.D., The Pennsylvania State University, 1999.
[38] X. He, S.M. Walton, B.T. Zigler, M.S. Wooldridge, A. Atreya, Experimental investigation of the intermediates of isooctane during ignition, Int. J. Chem. Kinet. 39 (2007) 498–517.
[39] T.S. Norton, F.L. Dryer, An experimental and modeling study of ethanol oxidation kinetics in an atmospheric pressure flow reactor, Int. J. Chem. Kinet. 24 (1992) 319–344.
[40] N. Leplat, P. Dagaut, C. Togbé, J. Vandooren, Numerical and experimental study of ethanol combustion and oxidation in laminar premixed flames and in jet-stirred reactor, Combustion and Flame. 158 (2011) 705–725.
[41] T.M. Foong, M.J. Brear, K.J. Morganti, G. da Silva, Y. Yang, F.L. Dryer, Modeling End-Gas Autoignition of Ethanol/Gasoline Surrogate Blends in the Cooperative Fuel Research Engine, Energy Fuels. 31 (2017) 2378–2389.

Appendix

Species profiles at 650 K

Species time-history concentrations and temperatures are measured for ethanol/iso-octane mixtures (E0, E10, E20, E50, E85, E100, by liquid vol%) at reactor temperatures of 650 K (Figures A.1-A.6) and 875 K (Figures A.7-A.12), pressure of 10 bar and equivalence ratio of 0.058. Kinetic simulations are performed using a gasoline surrogate model by Mehl et al. [27]. The dashed lines in these figures correspond to the open symbols. Note that the initial fall in the temperature profile is caused by an unheated section at the reactor entrance rather than endothermic reactions [19].

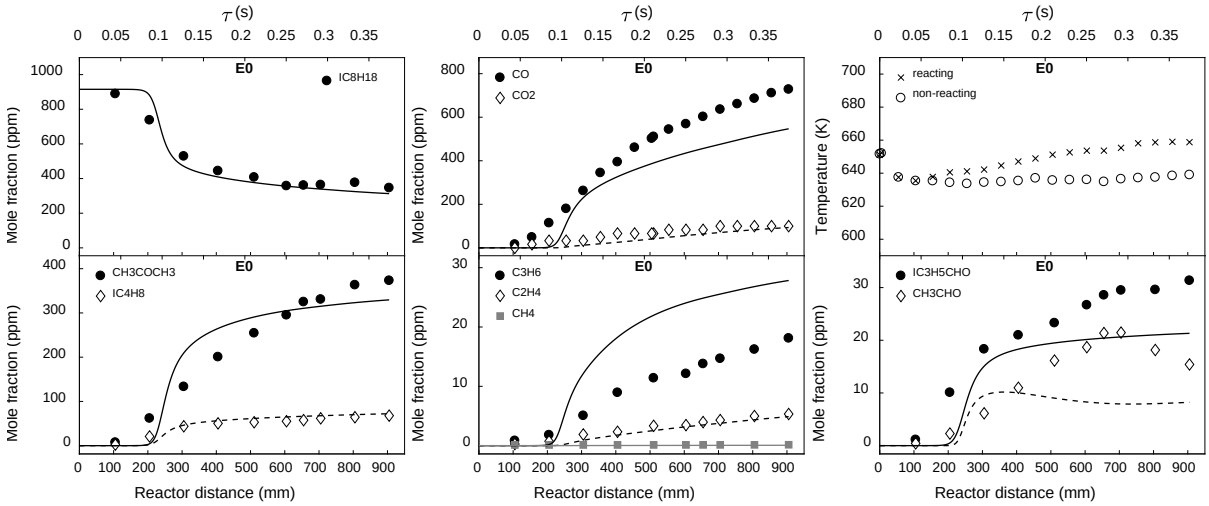

Figure A.1 Species and temperature profiles of E0 (iso-octane) oxidation in the flow reactor at 650 K, 10 bar, ϕ = 0.058.

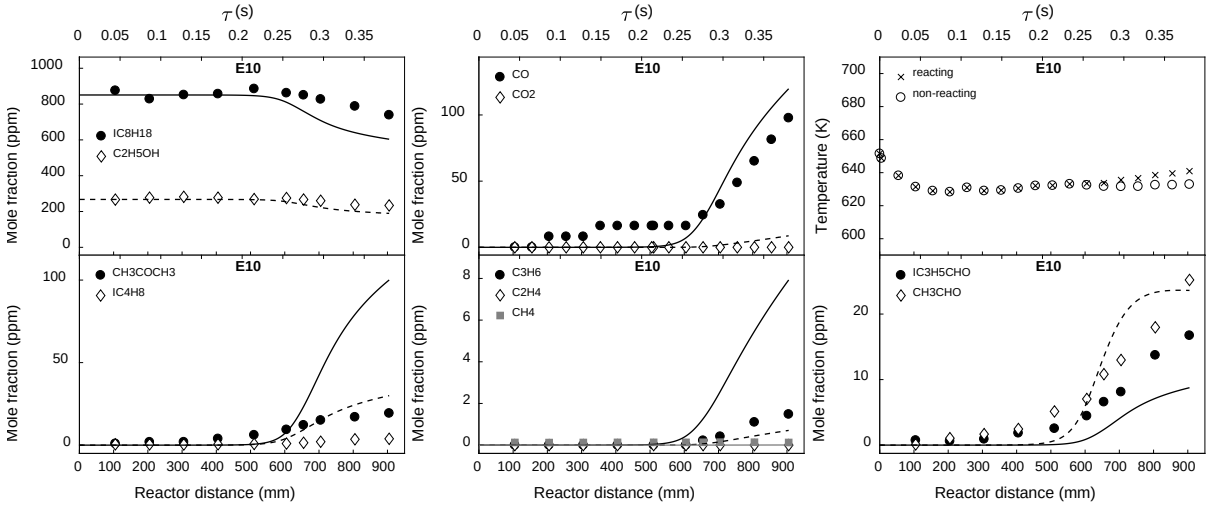

Figure A.2 Species and temperature profiles of E10 oxidation in the flow reactor at 650 K, 10 bar, ϕ = 0.058.

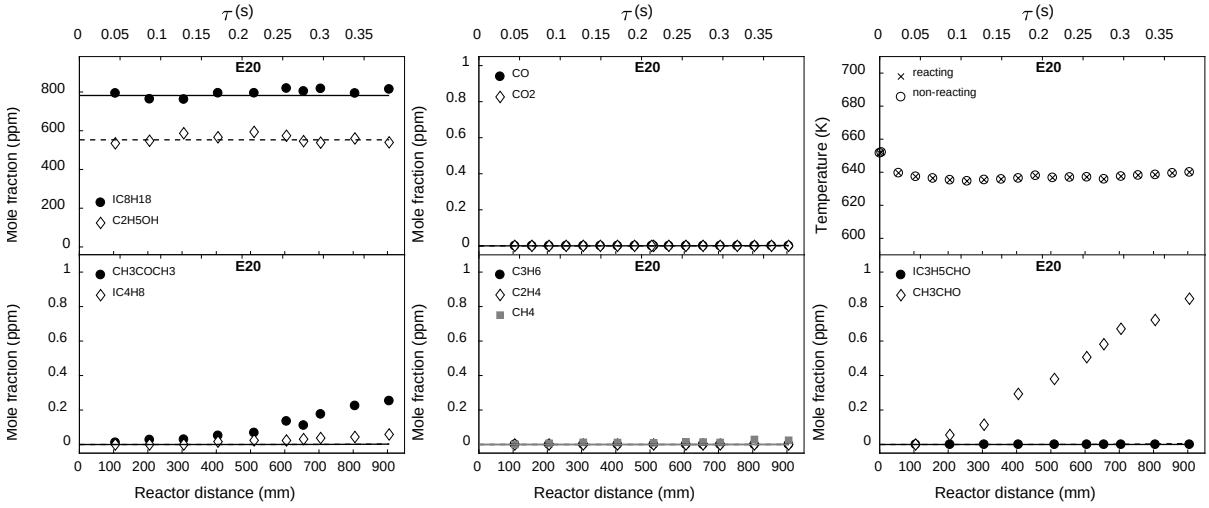

Figure A.3 Species and temperature profiles of E20 oxidation in the flow reactor at 650 K, 10 bar, ϕ = 0.058.

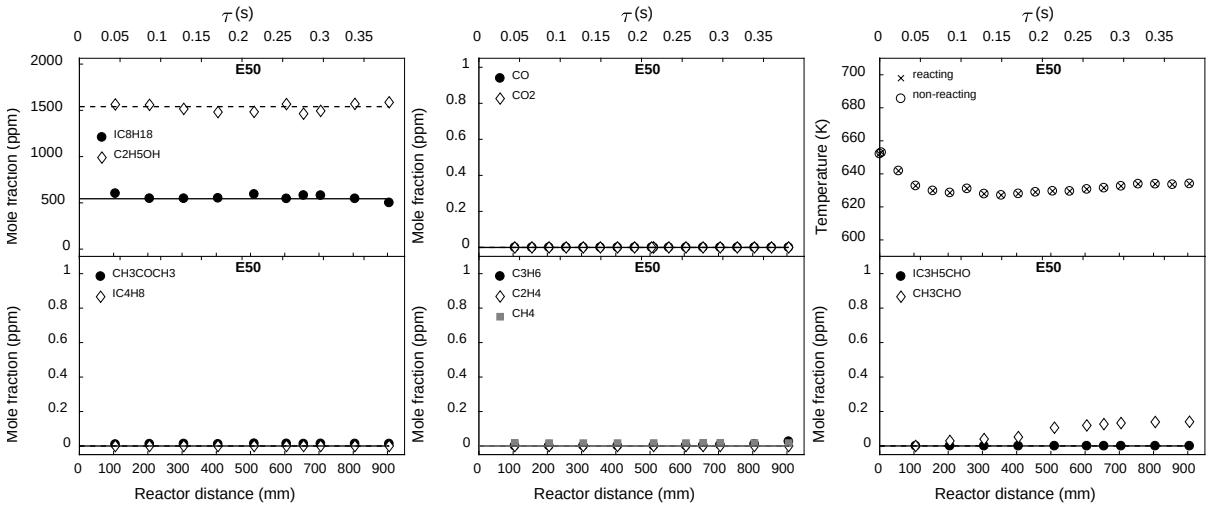

Figure A.4 Species and temperature profiles of E50 oxidation in the flow reactor at 650 K, 10 bar, ϕ = 0.058.

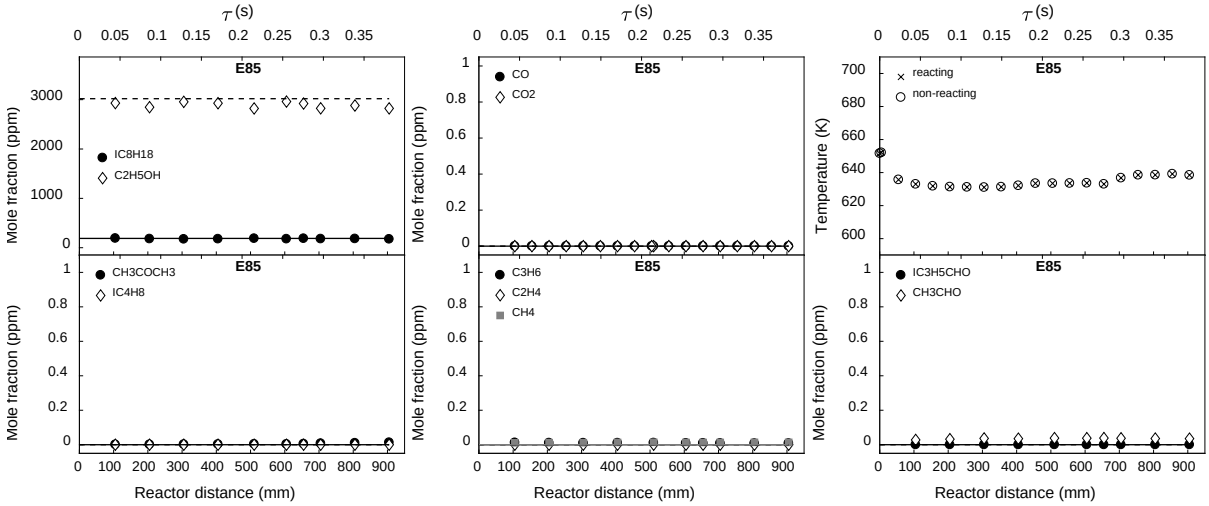

Figure A.5 Species and temperature profiles of E85 oxidation in the flow reactor at 650 K, 10 bar, ϕ = 0.058.

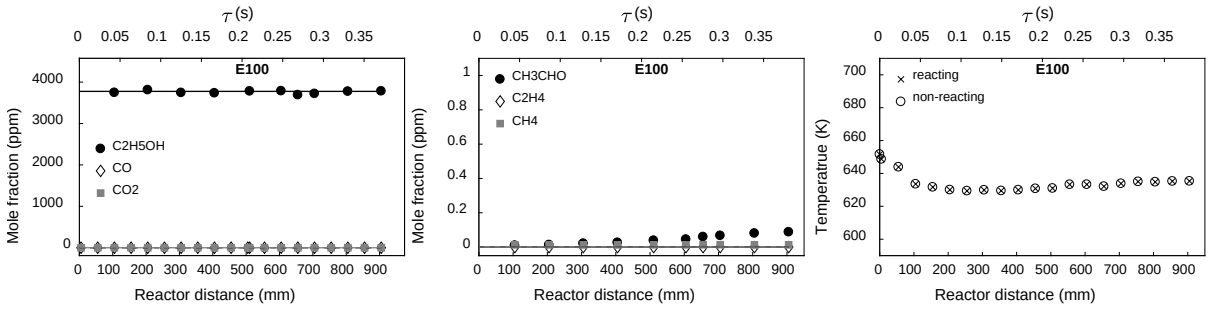

Figure A.6 Species and temperature profiles of E100 (ethanol) oxidation in the flow reactor at 650 K, 10 bar, ϕ = 0.058.

Species profiles at 875 K

Species time-history concentrations and temperatures are measured for ethanol/iso-octane mixtures (E0, E10, E20, E50, E85, E100, by liquid vol%) at reactor nominal temperature of 875 K, pressure of 10 bar and equivalence ratio of 0.058, as shown in Figure A.7 to Figure A.12. Kinetic simulations are performed using a gasoline surrogate model by Mehl et al. [33]. Dashed lines in these figures correspond to open symbols. Note that the initial drop in the temperature profile is caused by an unheated section at the reactor entrance instead of from endothermic reactions [25].

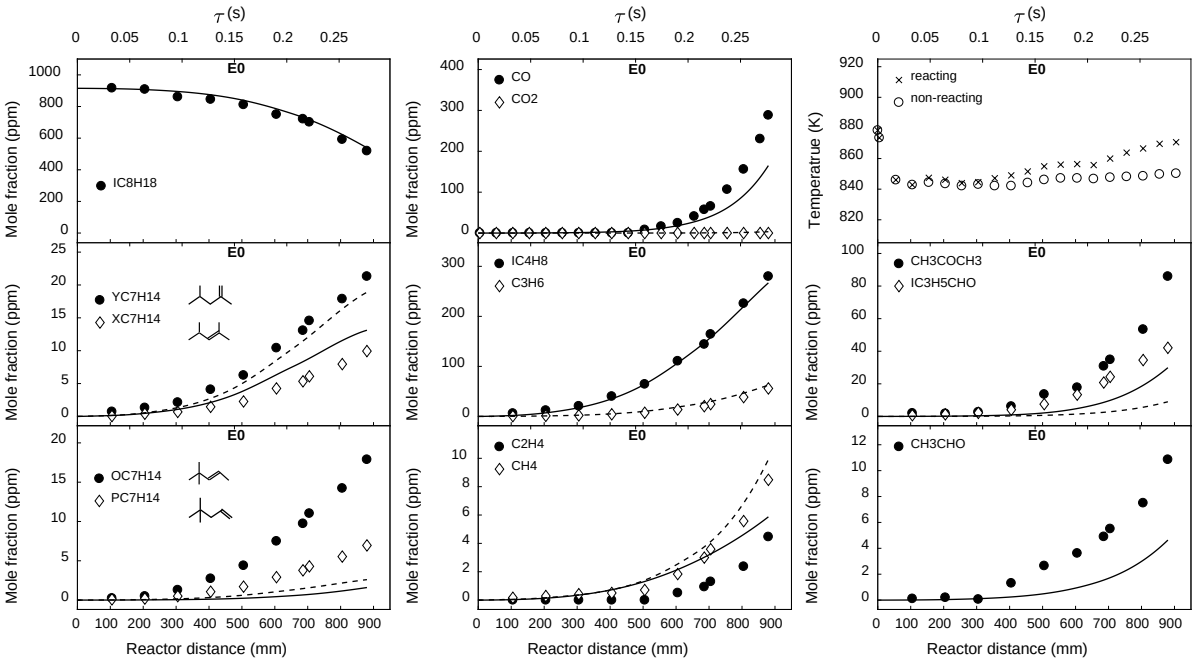

Figure A.7 Species and temperature profiles of E0 (iso-octane) oxidation in the flow reactor at 875 K, 10 bar, ϕ = 0.058.

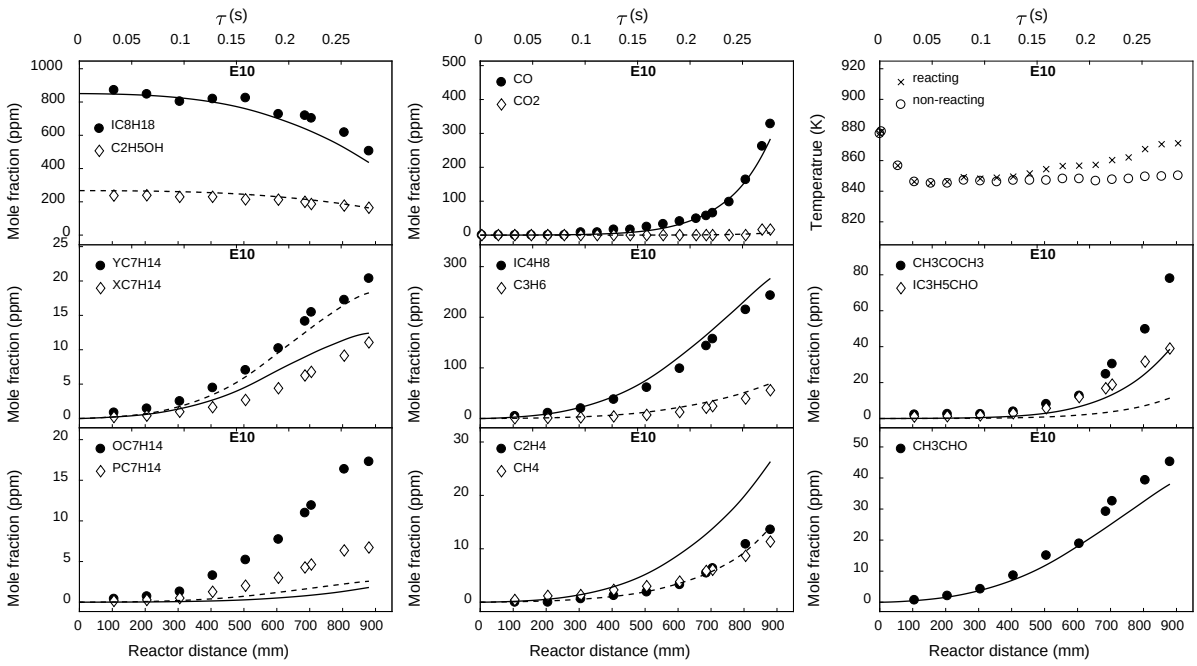

Figure A.8 Species and temperature profiles of E10 oxidation in the flow reactor at 875 K, 10 bar, ϕ = 0.058.

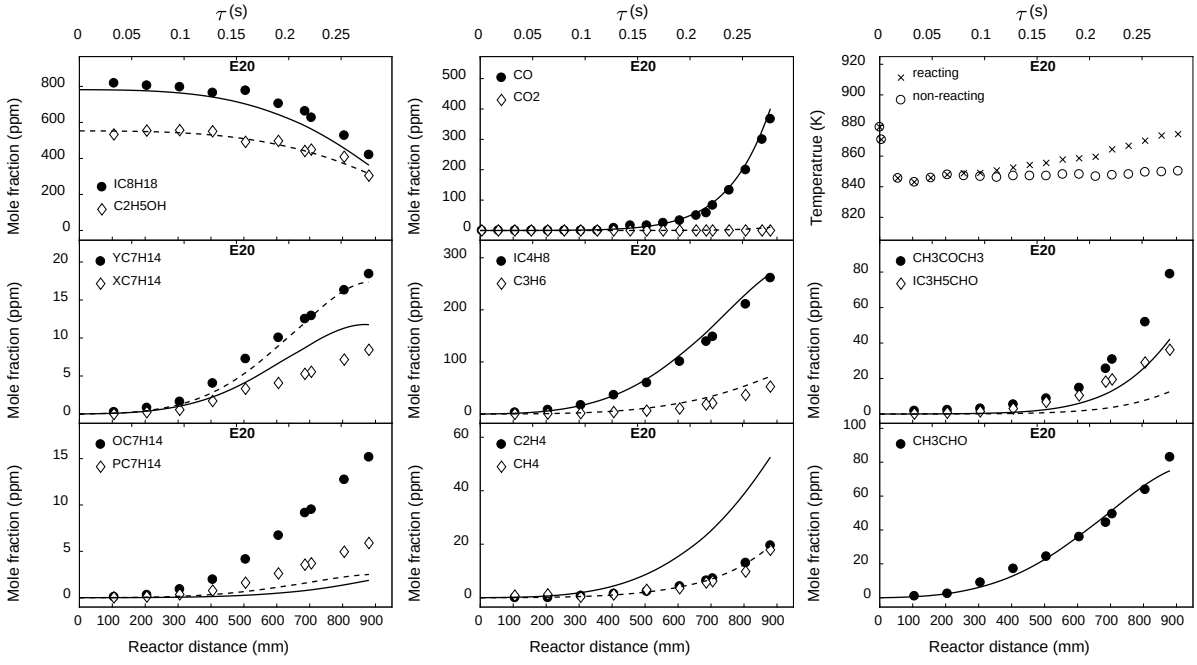

Figure A.9 Species and temperature profiles of E20 oxidation in the flow reactor at 875 K, 10 bar, ϕ = 0.058.

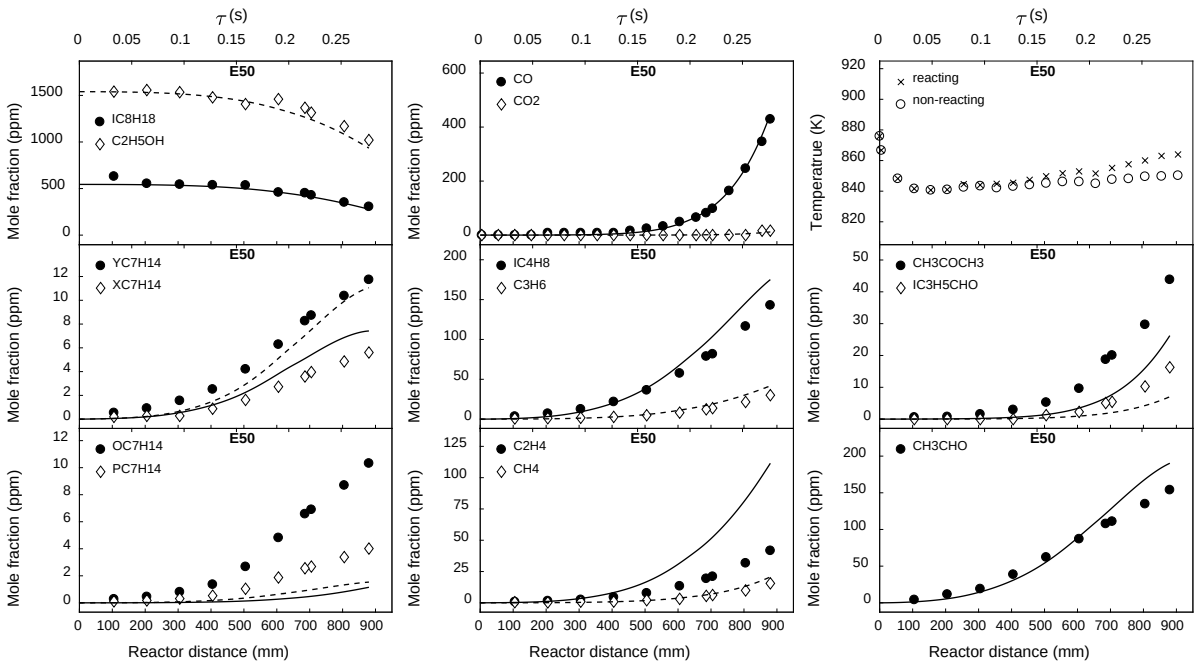

Figure A.10 Species and temperature profiles of E50 oxidation in the flow reactor at 875 K, 10 bar, ϕ = 0.058.

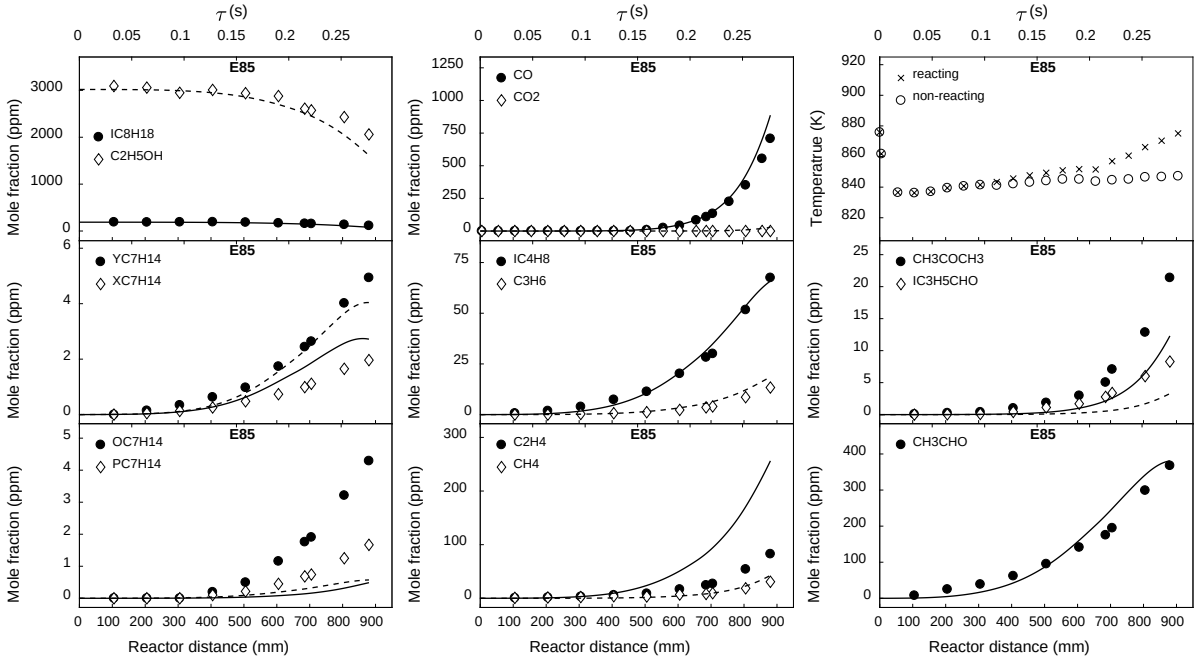

Figure A.11 Species and temperature profiles of E85 oxidation in the flow reactor at 875 K, 10 bar, ϕ = 0.058.

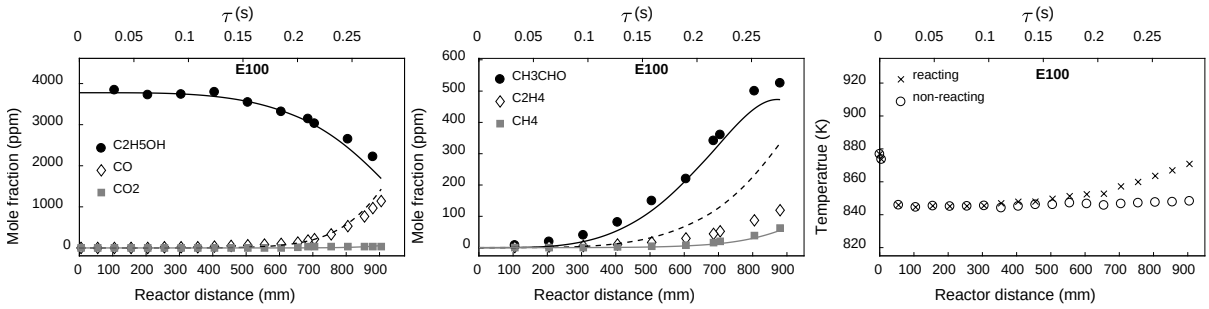

Figure A.12 Species and temperature profiles of E100 (ethanol) oxidation in the flow reactor at 875 K, 10 bar, ϕ = 0.058.